

The impact of water released from boehmite nanoparticles during curing in epoxy-based nanocomposites

Tassilo Waniek^{1,2}  | Ulrike Braun¹  | Dorothee Silbernagl¹  | Heinz Sturm^{1,2} 

¹Department 6 Materials Chemistry, Division 6.6 Physical and Chemical Analysis of Polymers, Bundesanstalt für Materialforschung und -prüfung (BAM), Berlin, Germany

²Faculty V of Mechanical Engineering and Transport Systems, Institute of Machine Tools and Factory Management (IWF), Tribology, Technical University of Berlin, Berlin, Germany

Correspondence

Tassilo Waniek, Bundesanstalt für Materialforschung und -prüfung (BAM), 12205 Berlin, Germany.
Email: tassilo.waniek@bam.de

Funding information

Deutsche Forschungsgemeinschaft, Grant/Award Number: FOR2021 “Acting principles of nanoscale matrix additives for composite structures”

Abstract

The enhancing effect on mechanical properties of boehmite (γ -AlOOH) nanoparticles (BNP) in epoxy-based nanocomposites on the macroscopic scale encouraged recent research to investigate the micro- and nanoscopic properties. Several studies presented different aspects relating to an alteration of the epoxy polymer network formation by the BNP with need for further experiments to identify the mode of action. With FTIR-spectroscopic methods this study identifies interactions of the BNP with the epoxy polymer matrix during the curing process as well as in the cured nanocomposite. The data reveals that not the BNP themselves, but the water released from them strongly influences the curing process by hydrolysis of the anhydride hardener or protonation of the amine accelerator. The changes of the curing processes are discussed in detail. The changes of the curing processes enable new explanation for the changed material properties by BNP discussed in recent research like a lowered glass transition temperature region (T_g) and an interphase formation.

KEYWORDS

composites, nanoparticles, nanowires and nanocrystals, spectroscopy, structure-property relationships, thermosets

1 | INTRODUCTION

Epoxy polymer composites are known for their wide range of applications from civil infrastructure to aircraft parts.^{1,2} Their durability, resilience and cost-efficiency is raised by incorporating inorganic additives. Additives that improve multiple properties are of special interest.³ One promising additive are boehmite (γ -AlOOH) nanoparticles (BNP) which has been shown to have a positive effect on many properties such as Young's modulus with an increase of up to 20%,⁴ fracture toughness (61%)⁴ and flame retardancy.^{5,6} Furthermore, it is nontoxic, commercially available and offers possibilities to be surface modified with, for example,

silanes according to its applications or surrounding matrix.^{7,8}

The enhancing effect of BNP in epoxy-based nanocomposites on the macroscopic scale encouraged recent research to investigation of the micro- and nanoscopic properties of the additive in epoxy-based nanocomposites. A detailed analysis by small- and wide-angle X-ray scattering determined that the crystalline structure of the BNP is unaffected by the incorporation into the epoxy polymer matrix,⁹ although the BNP have a tremendous impact on their surrounding epoxy polymer matrix. With high resolution force spectroscopy a significant difference in stiffness of the

This is an open access article under the terms of the Creative Commons Attribution-NonCommercial-NoDerivs License, which permits use and distribution in any medium, provided the original work is properly cited, the use is non-commercial and no modifications or adaptations are made.

© 2021 The Authors. *Journal of Applied Polymer Science* published by Wiley Periodicals LLC.

epoxy polymer matrix in vicinity of the BNP compared to the BNP itself and the epoxy matrix outside the particle range has been discovered.^{10,11} The significant influence of the BNP on the network formation is further supported by the observed changes in glass transition temperature region T_g . With rising BNP content, the overall T_g decreases up to 10 K.⁹ Thermomechanical analysis identified two distinct T_g that have been assigned to epoxy polymer within and outside the vicinity of the BNP.¹² These findings lead to the suggestions that BNP influence the curing processes by (i) hindering the diffusion during curing or (ii) altering the stoichiometry by bonding or absorbing one component of the resin system or (iii) initiating a different curing process, for example, catalyzed by the surficial hydroxyl-groups.^{9,10,12-14}

These suggestions are in agreement with other investigations which have shown an influence of the BNP on the epoxy network formation^{9,15} or proposed an influence of boehmite on the molecular scale.^{7,16} An additional aspect that has not been considered yet for epoxy-based nanocomposites is the possible influence of water present in the BNP.^{8,17} Recent research on boehmite reinforced polyamide or polysiloxane pointed out that water released from the BNP during the curing process has an influence on the polymer structure and properties.^{18,19}

A systematic FTIR-spectroscopic approach is chosen in this work to investigate interactions and reactions of the BNP and its present water with components of an anhydride cured epoxy resin during the curing process. The identified molecular behavior of this complex nanocomposite system is investigated and discussed regarding the fundamental knowledge of epoxy polymer curing processes with interest to identify the origin of the reinforcing effect induced by BNP.

2 | EXPERIMENTAL SECTION

2.1 | Chemicals and reagents

As matrix material, commercially available epoxy resin bisphenol A diglycidyl ether (DGEBA, Araldite[®] LY 556, Huntsman) cured with the anhydride hardener (AH) methyltetrahydrophthalic anhydride (MTHPA, Aradur[®] HY 917, Huntsman) and accelerator (Acc) 1-methylimidazole (1-MEI, DY 070, Huntsman) were used. Boehmite (γ -AlOOH) nanoparticles (BNP, DISPERAL HP14) with a primary particle size of 14 nm were kindly supplied by SASOL Germany GmbH. Dried BNP (dBNP) were prepared by treatment of as received BNP at 80°C for 5 h. Ultrapure water was used with electrical conductance of 0.055 $\mu\text{S}\cdot\text{cm}^{-1}$.

2.1.1 | Thermogravimetric analysis

Thermogravimetric analysis (TGA) was performed on the as received BNP and dBNP powders (STA7200, Hitachi High-Tech Analytical Science, Oxford, UK). 10 mg of each BNP were measured in alumina crucibles at a heating rate of 10 $\text{K}\cdot\text{min}^{-1}$ in nitrogen flow of 200 $\text{ml}\cdot\text{min}^{-1}$ up to 600°C and from 600 to 1000°C in synthetic air flow of 200 $\text{ml}\cdot\text{min}^{-1}$.

2.2 | Powder X-ray diffraction

Powder X-ray diffraction (XRD) data were collected for dBNP and as received BNP using a Bruker D8 Discover diffractometer (Bruker AXS, Germany) with a SolX-detector using Cu-K α 1 radiation ($\lambda = 1.540566 \text{ \AA}$) over a range of $2\theta = 5^\circ$ to 60° with a step size of 0.009° . The time per step was 0.6 s. The powder was packed onto a PVC sample holder which was mounted into the diffractometer.

2.3 | ATR-FTIR spectroscopy heating series

For the ATR-FTIR investigations the individual components of the epoxy system DGEBA, AH and Acc were investigated in pure form as well as manually mixed for 2 min with either 30 wt% of dBNP or with 30 wt% as received BNP or with 9.1 wt% water. 30 wt% BNP in DGEBA has been found a processable suspension to prepare epoxy samples.⁴ The water content of 9.1 wt% equals a stoichiometric amount regarding the BNP content. The mixtures were then heated to 80°C. Samples for ATR-FTIR spectroscopy were taken after 0, 15, 30, 60, and 120 min of heat treatment. ATR-FTIR spectroscopy was performed with a Nicolet 6700 equipped with SmartOrbit Diamond module and DTGS detector. The spectra were recorded from 4000 to 500 cm^{-1} averaging 32 scans with a resolution of 2 cm^{-1} . The obtained data were processed with ATR correction available with the OMNIC 9 software (Thermo Fischer Scientific, Karlsruhe, Germany).

2.4 | Near-infrared investigations of DGEBA with BNP

Near-infrared spectroscopy (NIR) was performed at 80°C on pure DGEBA, DGEBA with 30 wt% BNP and DGEBA with 9.1 wt% water. The BNP were dispersed in the DGEBA by a kneader and in a three-roller mill as described elsewhere in detail.²⁰ DGEBA was manually

mixed with water for 2 min. The DGEBA mixtures were applied into cuvettes of optical glass (Starna Scientific Limited, Essex, England, type: 1/G/1) of 1 mm layer thickness. The NIR measurements were recorded using a Nicolet 8700 FTIR spectrometer (Nicolet Instruments, Offenbach, Germany) in transmission mode using a white light source, a nitrogen cooled mercury cadmium telluride detector (MCT-A) and equipped with a heatable NIR Cell from Pike Technologies (Madison) modified by RESULTEC analytic equipment (Illerkirchberg, Germany).²¹ The set of spectra were recorded at 80°C from 7500 to 4000 cm^{-1} with a resolution of 4 cm^{-1} averaging 32 scans with a time interval of 12.5 s per spectrum.

2.5 | Investigation of the nanocomposite with DRIFTS

The bulk samples of boehmite-reinforced epoxy-based nanocomposite with a BNP content of 0, 5, 10, and 15 wt % were prepared as described by Jux et al.⁴

For DRIFT spectroscopy the nanocomposite bulk samples were grinded with a Retsch CryoMill in a 50 ml milling mug. The mug was filled 2/3 with pieces of the nanocomposites and a 25 mm steel grinding ball. After 10 min of pre-cooling with liquid nitrogen three milling cycles à 5 min at 25 Hz paused for 30 s at 5 Hz after each cycle were run. Next, 15 mg of the milled neat epoxy polymer or nanocomposite was mixed with potassium bromide (KBr for IR spectroscopy, ROTH) and grinded with pestle and mortar. The KBr mixtures were measured with a Nicolet 8700 FTIR spectrometer equipped with the DRIFT module Praying Mantis™ with DRP-SAP sampling kit by Harrick Scientific and an MCT-A detector. The spectra were recorded from 4000 to 500 cm^{-1} averaging 32 scans with a resolution of 2 cm^{-1} . For better comparison the recorded spectra were normalized to their absorbance maximum at 1740 cm^{-1} and the baseline was corrected to their minimum.

3 | RESULTS

Different FTIR-spectroscopic experiments were chosen to investigate the interactions and reactions of the boehmite nanoparticles (BNP) in epoxy-based nanocomposites. This chapter presents the molecular changes induced by the BNP and water released from them on the anhydride hardener (AH), amine accelerator (Acc) or epoxy resin (DGEBA) during thermal curing at 80°C and in the cured epoxy polymer (Ep). The impact of these molecular changes on the curing process, network formation and material properties are considered in the chapter of Discussion.

To differentiate between the effects of water and the BNP, the individual neat components listed in the resin

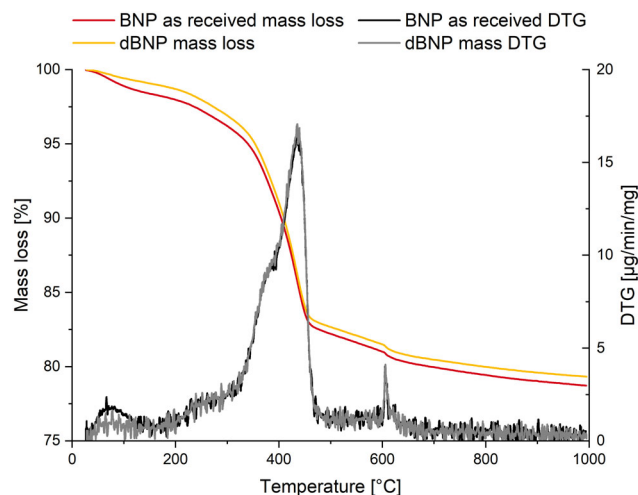


FIGURE 1 TGA-profiles for dried and as received BNP [Color figure can be viewed at wileyonlinelibrary.com]

system (AH, Acc or DGEBA) were mixed with BNP, water (H_2O) and dried BNP (dBNP) that are nearly waterfree, respectively. After heat treatment at 80 °C the mixtures were analyzed by ATR-FTIR spectroscopy.

3.1 | Composition of dried BNP

The composition of the BNP needs to be considered to understand their influence on the components of the resin system. BNP ($\gamma\text{-AlOOH}$) have a layered orthorhombic crystal structure with hydroxyl-groups on the surface and contain a considerable amount of water.^{17,18,23} It has been determined by XRD that dBNP have the same crystal structure as the as received BNP (see SI Figure S1). TGA revealed that dBNP have a significantly lower water content compared to as received BNP especially at the curing temperatures of 80 and 120°C (Figure 1 and Table 1).

3.2 | Hardener MTHPA HY 917

Changes of the AH under curing conditions (80°C) due to the presence of BNP (AH + BNP), dBNP (AH + dBNP), and water (AH + H_2O) were investigated with ATR-FTIR spectroscopy. The most significant difference is visible in the region of the carbonyl stretch as depicted for the mixtures treated for 30 min at 80°C in Figure 2. For mixtures of AH + BNP or AH + H_2O an additional carbonyl peak at 1711 cm^{-1} appears clearly and is already visible after 15 min at 80°C (see Figure S4 and S5). This peak is not observed in the spectrum of pure AH nor AH + dBNP. The absence of the signal at 1711 cm^{-1} for AH + dBNP compared to AH + BNP

TABLE 1 Percentage mass loss of as received and dried BNP

Mass loss at in %	80°C pre-curing	120°C post-curing	300°C before transformation to $\gamma\text{-Al}_2\text{O}_3$ ²²	600°C before transformation to $\delta\text{-Al}_2\text{O}_3$ ²²
BNP	0.78	1.34	3.80	18.99
Dried BNP	0.41	0.73	3.09	18.50

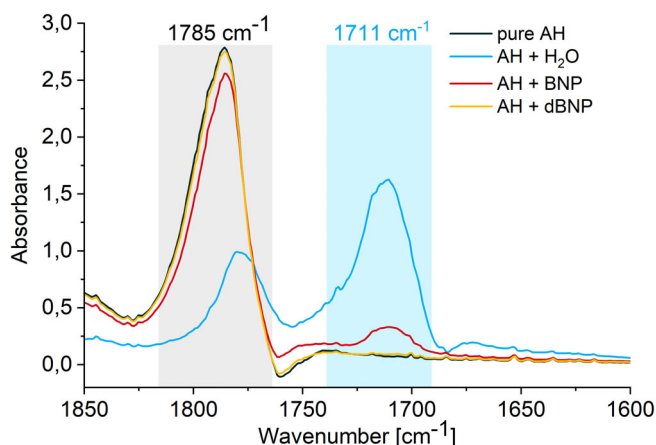


FIGURE 2 ATR-FTIR spectra of heated (80°C, 30 min) anhydride hardener pure (pure AH), with water (AH + H₂O), BNP (AH + BNP), or dBNP (AH + dBNP). The shifted band from 1785 to 1711 cm⁻¹ suggests a reaction between water released from the BNP and the AH as depicted in Figure 3. Due to phase separation only the signals of AH species are visible and no signals of water [Color figure can be viewed at wileyonlinelibrary.com]

reveals that the additional peak is not caused by an interaction of the AH with the BNP. Regarding that water with hardener (AH + H₂O) shows the signal at 1711 cm⁻¹, the hydrolysis of the AH by water released from the BNP under curing conditions (80°C) is conclusive (Figure 3).

The significant differences of the absorbance between AH + BNP and AH + H₂O at around 1785 and 1711 cm⁻¹ can be correlated with the amounts of present water in the mixtures. While AH + H₂O contains 9.1 wt% water what equals a molar ratio of approx. 1:1, AH + BNP contains 30 wt% BNP resulting in only 0.48 wt% water what equals a molar ratio of approx. 100:7 (AH:H₂O).⁸ Therefore, the hydrolysis of the AH by BNP is partial. A partial hydrolysis of the AH in a resin system alters the curing process and the properties of the cured epoxy polymer.^{25,26} To understand the influence of the BNP, their influence on all single components of the resin system need to be investigated. The results of all investigations and their impact on the curing process is considered in the Chapter of Discussion.

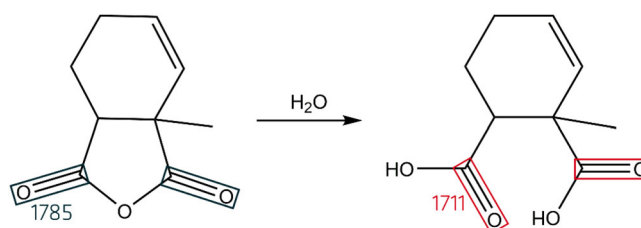


FIGURE 3 Reaction of anhydride hardener (AH) and water with assigned carbonyl absorption bands in cm⁻¹ ²⁴ [Color figure can be viewed at wileyonlinelibrary.com]

3.3 | Accelerator 1-MEI DY 070

Analogue to the investigations of the other components of the resin system, mixtures of the amine accelerator (Acc) with BNP, dBNP and water were investigated with ATR-FTIR spectroscopy after treatment at curing conditions (80°C, Figure 4). As was observed for AH additional peaks appear for Acc + H₂O and Acc + BNP compared to the pure Acc and Acc + dBNP. Acc + BNP shows a shoulder or small peak at 908 cm⁻¹ near the 912 cm⁻¹ peak of pure Acc and a significantly higher signal around 3400 cm⁻¹ that is not only related to boehmites broad signals around 3100 and 3300 cm⁻¹. For the mixture of Acc + H₂O the peaks at 741 and 819 cm⁻¹ are slightly shifted to higher wave numbers. Furthermore, the peaks at 912 and 908 cm⁻¹ have the same intensity. Furthermore, the peak at 1520 cm⁻¹ appears to be less intense than for pure Acc and broad bands appeared around 1670 and 3400 cm⁻¹.²⁷

The additional peaks observed for Acc + H₂O are explainable by the molecular structure of the Acc 1-Methylimidazol (1-MEI) as illustrated in Figure 5. The pK_s of 1-MEI is 6.95 meaning that this molecule is protonated by water until the reaction is in equilibrium.²⁸ Due to the equilibrium state it is possible that the signals at 1670 and 3400 cm⁻¹ are overlaid by water signals at 1640 and 3450 cm⁻¹ but not the other new bands. For small amounts of water as that is released from the BNP, only peaks with high absorbance at 912 and 3400 cm⁻¹ of the new species become visible. Therefore, the mixture of accelerator with BNP (Acc + BNP) as shown in Figure 4 exhibits only some peaks of the protonated

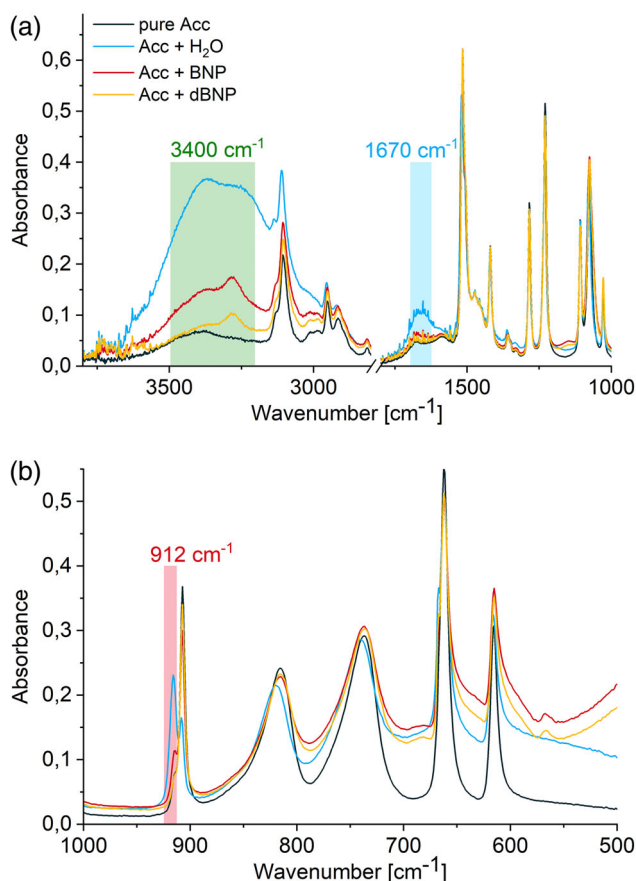


FIGURE 4 (a) and (b) ATR-FTIR spectra of heated (80°C, 30 min) amine accelerator (Acc) - pure (pure Acc, black), with water (Acc + H₂O, blue), BNP (Acc + BNP, red), or dBNP (Acc + dBNP, yellow). The additional absorption bands for Acc + BNP and Acc + H₂O compared to pure Acc and Acc with dBNP suggesting the reaction between Acc and water released from the BNP as depicted in Figure 5 and described in Table 2 [Color figure can be viewed at wileyonlinelibrary.com]

TABLE 2 Assignments of FTIR bands of pure Acc 1-MEI and protonated form H1-MEI (see Figure 5)²⁹

Wave number in cm ⁻¹	Stretching
3400	$\nu_{\text{N-H}}$ of secondary amine next to located double bond in H1-MEI
1670	Stretch of isolated double bonds in H1-MEI
1520	Stretching of aromatic ring in pure 1-MEI
912	$\gamma_{\text{C-H}}$ between N-atoms H1-MEI
908	$\gamma_{\text{C-H}}$ between N-atoms in 1-MEI
819 and 741	Other $\gamma_{\text{C-H}}$ in imidazole ring slightly shifted for H1-MEI due to changed electron distribution compared to 1-MEI

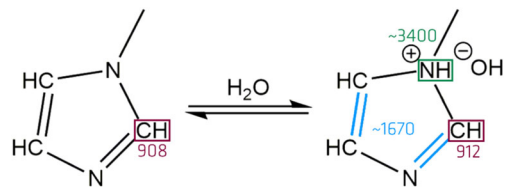


FIGURE 5 Structure of pure Acc 1-MEI (left) and protonated form H1-MEI (right) with assigned changing bands in cm⁻¹ [Color figure can be viewed at wileyonlinelibrary.com]

species that becomes fully visible for the mixture of Acc with water (Acc + H₂O). The new signals for the protonated species are related to new peaks described in Table 2 and Figure 5.

No differences are visible the FTIR-spectra of Acc and Acc + dBNP Figure 4 except for signals related to the BNP itself.²⁷ Therefore, a protonation by water released from as received BNP (Acc + BNP) of the Acc (1-MEI) is conclusive. The protonation happens during the curing reaction within less than 15 min (see Figure S8 and S9). This fast protonation can have a huge impact on the network formation because the initial nucleophilic attack of the tertiary amine 1-MEI during the polymerization is inhibited by the proton.²¹ Instead, the polymerization can be initiated by the formed hydroxide or a complex formed between Acc, water and AH.^{30,31} Further influence on the curing process and thereby, material properties are considered in the Chapter of Discussion.

3.4 | Epoxy resin DGEBA LY 556

The same investigations as for the AH and Acc were performed for the epoxy resin DGEBA. Contrary to the other components neither BNP nor dBNP nor water showed any additional or shifted signals by ATR-FTIR investigation after treatment at 80°C for 120 min (See Figure S11, S12 and S13). An interaction or reaction of water or BNP with the network forming epoxy group of the DGEBA should lead to a shift of or shoulder at the peak at 3056 cm⁻¹ related to the symmetric C—H stretching of the oxirane ring as well as a broad band around 3600 cm⁻¹ assigned to an O—H stretching.^{29,32} Both were not observable.

Additionally, the DGEBA mixed with either as received BNP or water was investigated in the near-infrared region in transmission mode but did not show any evidence. The results finalize the evidence that the DGEBA is neither affected by the BNP nor water released from it. The obtained results question suggestions from the literature.

Abliz et al. performed calorimetric analysis of BNP in DGEBA.¹⁵ Their analysis revealed an exothermic peak in the first heating starting at 100°C and a slight raise of the glass transition temperature region in the second heating. This shift was related to the suggested reaction of the epoxy groups with the BNP surface as described by Exner et al.⁷ The suggestion is based on a plausible argumentation but requires further validation even through the authors mind. The observed reactivity of water released from the BNP with the AH and Acc is expected to be the predominant influence on the curing processes. The influence of BNP on DGEBA is neglected in the following discussions.

3.5 | Cured boehmite-reinforced epoxy-based nanocomposite

For the comparison of neat cured epoxy polymer (Ep) with BNP reinforced nanocomposites (Ep + 15BNP) DRIFT-spectroscopy of cryomilled samples was used. It is a highly suitable method to analyze solid samples avoiding effects due to scattering, refraction or sample its geometry compared to other infrared spectroscopic methods. Additionally, the cryomilling was found to be the best preparation method to target all phenomena without lack of penetration depth or statistical distribution.²⁹

Figure 6 represents the DRIFT spectra of Ep and Ep + 15BNP. One can observe that the most obvious differences in the spectra of Ep and Ep + 15BNP are related to the BNP presence (full spectra can be found in Figure S14).²⁷ A closer look at the signals related to the epoxy polymer shows that they are the same except for

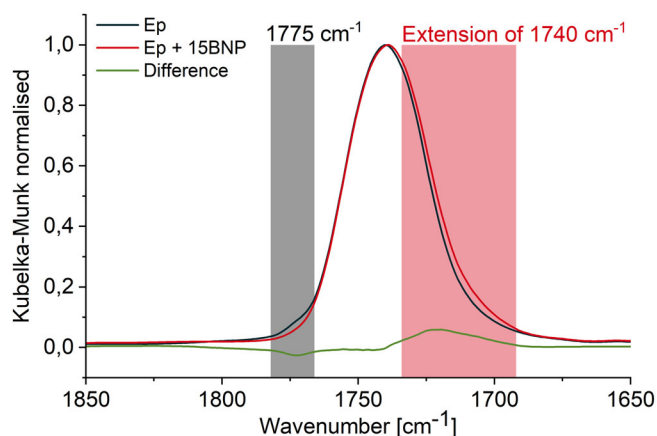


FIGURE 6 DRIFT spectra of cryomilled samples in KBr: Cured epoxy polymer pure (ep, black), nanocomposite with 15 wt% BNP (ep + 15 BNP, red) and their difference (green). Showing an influence of the BNP in the nanocomposite by a missing shoulder at 1775 cm⁻¹ and an extension of the carbonyl peak at 1740 cm⁻¹ [Color figure can be viewed at wileyonlinelibrary.com]

the range between 1850 and 1650 cm⁻¹ (Figure 6). This range is related to the carbonyl stretch.^{29,33} One difference is an extension of the peak at 1740 cm⁻¹ to lower wave numbers for BNP reinforced samples although the maximum is not shifted. This peak extension to lower wave number can be assigned to hydrolyzed hardener as described in the previous section on AH and depicted in Figure 3. Another difference is the shoulder at 1775 cm⁻¹ for Ep after the onset of the peak at 1740 cm⁻¹ which is clearly visible for Ep but barely recognizable for a BNP content of 15 wt% (Ep + 15BNP). Steinmann et al. related the shoulder at 1775 cm⁻¹ to chain anhydride formed by homopolymerisation of AH as a side reaction of alternating esterification. Whereas the chain anhydride formation depends on the concentration of the Acc and is influenced by humidity.³⁴ This supports the previous finding that the Acc is protonated by water released from the BNP.

4 | DISCUSSION

The analysis with different FTIR-spectroscopic methods shows that an important impact of the BNP is induced by its present water released under curing conditions.^{17,18} Although the surficial hydroxyl-groups of BNP in epoxy-based nanocomposites might be able to locally change the curing processes in various ways, their impact is neglected in the following consideration.^{13,24,35,36} The impact of water released from the BNP is so predominant that the influence of water-free BNP need to be investigated separately.

To get an insight on the properties of BNP-reinforced epoxy-based nanocomposites the changes in the curing process and network formation by water need to be discussed. Depending on the amount of water, different curing processes are possible (see Table 3). The water-free process A, processes in the presence of low amount of water leading to the processes B and C or bigger amounts of water causing the process D. As discussed before the DGEBA is expected to be unchanged by BNP (see section on DGEBA in Results).

Even with controlled conditioning the process of curing epoxy resins with anhydride hardener and amine accelerator is not fully understood.³⁴ Therefore, this discussion focuses on pointing out differences induced by water released from the BNP and its influence on the material properties. A crucial step in the curing process is the initiation of the polymerization. After initiation an anion is formed that leads to polymerization (Figure 7).^{21,37}

The water-free catalyzed process A and the proton donor co-catalyzed curing process B are the most commonly and extensively discussed processes for amine

TABLE 3 Plausible curing processes A, B, C and D for BNP-reinforced epoxy-based nanocomposites

No.	Description	Hydrolyzed hardener	Protonated accelerator	Possible location
A	Water-free catalyzed	No	No	Neat epoxy polymer, outside range of BNP
B	Proton donor co-catalyzed	No	Yes	Vicinity of BNP, influence of humidity
C	Catalyzed esterification	Yes	No	Vicinity of BNP, influence of humidity
D	Uncatalyzed esterification	Yes	Yes	Vicinity of BNP

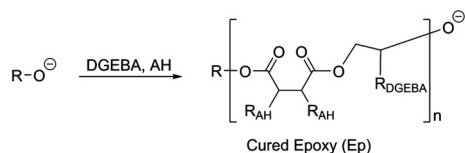


FIGURE 7 Reaction scheme of anionic polymerization after initiation of the curing process ($R = \text{AH}$ or DGEBA) monomer after initiation of polymerization³⁷

catalyzed, anhydride cured epoxy resin. The polymerization in water-free curing process A is initiated by an ionic activation due to a nucleophilic attack of the Acc either on the DGEBA or AH followed by an anionic polymerization (Figure 8).^{37,38} This curing process A is favorable for pristine educts under inert conditions.³⁴ A unique sign for curing process A is an absorption band at 1775 cm^{-1} representing segments formed by AH homopolymerisation instead of alternated polymerization of AH and DGEBA.^{34,39} The signal at 1775 cm^{-1} has mainly been observed for neat epoxy polymer and its absence in BNP reinforced epoxy-based nanocomposites is a clear sign for the presence of other curing processes.

In the presence of water as for curing exposed to air or in vicinity of BNP the reactants for curing process B or C are formed.³⁴ Process B is well known as proton donor co-catalyzed curing process although the detailed process remains unclear (Figure 9).^{30,31,38} The reaction enthalpy for process B is known to be lower than for process A.³⁰ Therefore the lower reaction enthalpy for BNP filled resin system detected by calorimetric measurements is a clear sign for the rising presence of this process with increasing BNP content.¹⁵

Curing process C was described in literature as well (Figure 10).^{25,40} The amine Acc can deprotonate the hydrolyzed hardener creating an anion like the initiating species in process A. In case of anhydride hydrolysis, the question remains how much hardener is hydrolyzed in the vicinity of the BNP. If huge amounts of hardener are locally hydrolyzed a chain growth for curing process C is impossible because it requires pristine anhydride hardener. A homopolymerisation of the DGEBA is unlikely due to the low curing temperature of 80°C .³¹ Therefore curing process C occurs only for low water content.

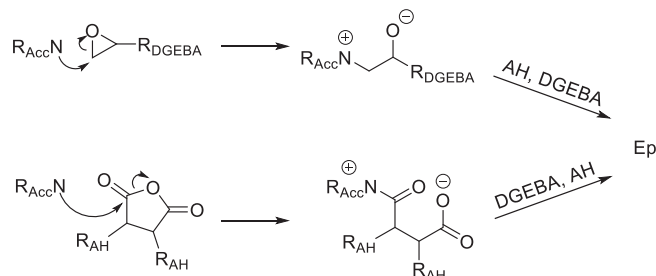


FIGURE 8 Water-free curing process A. initiation of the chain growth by nucleophilic attack of the Acc on the DGEBA or AH³⁷

Otherwise, if more water is present the protonation of the Acc and hydrolysis of the hardener leading to curing process D (Figure 11) is expected.

Curing process D does not offer the possibility to create a polymerization initiating anion (Figure 11). Therefore, only an uncatalyzed polyesterification might occur.^{41,42} Due to the low curing temperature (80°C) this process D is hindered.^{34,40}

To sum up the network forming curing processes can be divided into the categories water-free amine catalyzed (process A) and amine catalyzed with influence of water (process B and C). This opens the question how these curing processes influence the material properties. Water is known to decrease the glass transitions temperature region T_g .²⁶ Investigations, performed with the epoxy samples from the identical batch as in this work, revealed an overall lowered T_g with rising BNP content in differential scanning calorimetry (DSC) measurements⁹ and dynamic mechanical thermal analysis (DMTA) show the formation of epoxy polymer networks with two different T_g .¹² Although the individual components of the resin system do not contain any water by formulation, the common preparation at ambient conditions enables an influence of humidity even in the neat epoxy polymer.^{4,26,34} With rising BNP content the curing processes are predominantly influenced by water released from the BNP leading to a preferred formation of networks with the lower T_g .^{9,12} The preferred formation of networks with lower T_g is assignable to a wider presence of the curing processes B and C that are influenced by water released from the BNP.

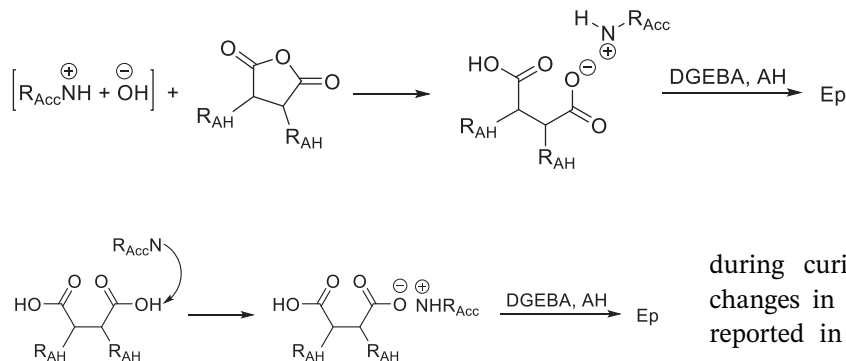


FIGURE 9 Proton donor co-catalyzed curing process B. the initiating step is catalyzed by interaction of the Acc with a proton donor like water³⁰

FIGURE 10 Catalyzed esterification curing process C. the curing is initiated by a hardener anion formed by deprotonation of the hydrolyzed AH²⁵

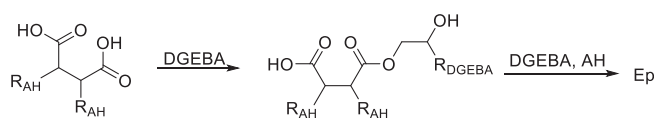


FIGURE 11 Uncatalyzed curing process D. this esterification does not occur due to curing temperature of 80°C⁴¹

Knowing the origin of the lowered T_g it can be estimated that the water released from BNP causes interphases of lower stiffness compared to the unaffected epoxy polymer in vicinity of the BNP as observed by high resolution force spectroscopy.¹⁰ Unlike the BNP which tend to form agglomerates⁴³ up to μm -size a small molecule like water is mobile and thereby able to influence the curing of the epoxy polymer not only close to the particle surface like a surficial hydroxyl group but in vicinity of the BNP.¹³

5 | CONCLUSION

Boehmite nanoparticle (BNP) reinforced epoxy-based nanocomposites were investigated with an FTIR-spectroscopic approach to identify the origins of property changes in the material. The effect of water released from the BNP on the curing processes could be identified as even more predominant than the BNP themselves. Analysis revealed a hydrolysis of the anhydride hardener (AH) and a protonation of the amine accelerator (Acc) in presence of as received BNP but not for dried BNP. The impact of water leads to an alteration of the curing processes. The water-free, amine catalyzed process A (Figure 8) and water co-catalyzed processes B and C (Figure 10 and Figure 11) define the network formation

during curing of the nanocomposite. The described changes in the curing processes match with properties reported in literature for BNP reinforced epoxy-based nanocomposites.

ACKNOWLEDGMENT

The work was funded by Deutsche Forschungsgemeinschaft (DFG) in the frame of the research unit FOR2021: “Acting principles of nanoscale matrix additives for composite structures”. The authors gratefully acknowledge Maximilian Jux at Technical University of Braunschweig for providing the nanocomposite samples, Benedikt Finke from Institute for Particle Technology Braunschweig for preparing the BNP/DGEBA-mixtures, Arielle Rieck for performing IR experiments, Marc Benjamin Hahn and Tihomir Solomun from BAM for advice on the IR data and Karina Fast from BAM for designing the graphical abstract.

ORCID

Tassilo Waniek <https://orcid.org/0000-0003-1089-2084>

Ulrike Braun <https://orcid.org/0000-0002-3682-3637>

Dorothee Silbernagl <https://orcid.org/0000-0001-8572-3184>

Heinz Sturm <https://orcid.org/0000-0002-8091-4077>

REFERENCES

- [1] C. Soutis, *Prog. Aerosp. Sci.* **2005**, *41*, 143.
- [2] L. C. Hollaway, *Constr. Build. Mater.* **2010**, *24*, 2419.
- [3] Y. Tang, L. Ye, Z. Zhang, K. Friedrich, *Compos. Sci. Technol.* **2013**, *86*, 26.
- [4] M. Jux, J. Fankhänel, B. Daum, T. Mahrholz, M. Sinapius, R. Rolfes, *Polymer* **2018**, *141*, 34.
- [5] A. Sut, S. Greiser, C. Jäger, B. Schartel, *J. Therm. Anal. Calorim.* **2017**, *128*, 141.
- [6] J. Karger-Kocsis, L. Lendvai, *J. Appl. Polym. Sci.* **2017**, *135*, 45573.
- [7] W. Exner, C. Arlt, T. Mahrholz, U. Riedel, M. Sinapius, *Compos. Sci. Technol.* **2012**, *72*, 1153.
- [8] A. Zarinwall, T. Waniek, R. Saadat, U. Braun, H. Sturm, G. Garnweitner, *Langmuir* **2021**, *37*, 171.
- [9] P. Szymoniak, B. R. Pauw, X. Qu, A. Schönhals, *Soft Matter* **2020**, *16*, 5406.
- [10] M. G. Z. Khorasani, D. Silbernagl, D. Platz, H. Sturm, *Polymers* **2019**, *11*, 235.
- [11] N. Cano Murillo, M. G. Z. Khorasani, D. Silbernagl, M. B. Hahn, V.-D. Hodoroaba, H. Sturm, *J. Appl. Polym. Sci.* **2021**, *138*, 50231.

- [12] M. G. Z. Khorasani, D. Silbernagl, P. Szymoniak, V.-D. Hodoroaba, H. Sturm, *Polymer* **2019**, *164*, 174.
- [13] J. Baller, M. Thomassey, M. Ziehmer, R. Sanctuary, *Thermochim. Acta* **2011**, *517*, 34.
- [14] H. Kollek, *Int. J. Adhes. Adhes.* **1985**, *5*, 75.
- [15] D. Abliz, T. Jürgens, T. Artys, G. Ziegmann, *Thermochim. Acta* **2018**, *669*, 30.
- [16] J. Fankhänel, D. Silbernagl, M. G. Z. Khorasani, B. Daum, A. Kempe, H. Sturm, R. Rolfes, *J. Nanomater.* **2016**, *2016*, 1.
- [17] M. Nguefack, A. F. Popa, S. Rossignol, C. Kappenstein, *Phys. Chem. Chem. Phys.* **2003**, *5*, 4279.
- [18] G. N. Tomara, P. K. Karahaliou, D. L. Anastassopoulos, S. N. Georga, C. A. Krontiras, J. Karger-Kocsis, *Polym. Int.* **2019**, *68*, 871.
- [19] I. Topolniak, V.-D. Hodoroaba, D. Pfeifer, U. Braun, H. Sturm, *Materials* **2019**, *12*, 1513.
- [20] B. Finke, H. Nolte, C. Schilde, A. Kwade, *Chem. Eng. Res. Des.* **2019**, *141*, 56.
- [21] E. Duemichen, M. Javdanitehran, M. Erdmann, V. Trappe, H. Sturm, U. Braun, G. Ziegmann, *Thermochim. Acta* **2015**, *616*, 49.
- [22] M. Digne, P. Sautet, P. Raybaud, H. Toulhoat, E. Artacho, *J. Phys. Chem. B* **2002**, *106*, 5155.
- [23] J. T. Klopogge, L. V. Duong, B. J. Wood, R. L. Frost, *J. Colloid Interface Sci.* **2006**, *296*, 572.
- [24] B. V. MELE, E. Verdonck, *Compos. Interfaces* **1995**, *3*, 101.
- [25] X. Fernández-Francos, X. Ramis, À. Serra, *J. Polym. Sci., Part A: Polym. Chem.* **2014**, *52*, 61.
- [26] K. S. Chian, S. H. Lim, S. Yi, W. T. Chen, International Symposium on Electronic Materials and Packaging (EMAP2000), 289–296. **2000**
- [27] A. Ghorbani-Choghamarani, A. Ashraf Derakhshan, M. Hajjami, L. Rajabi, *RSC Adv.* **2016**, *6*, 94314.
- [28] D. R. Lide, *CRC Handbook of Chemistry and Physics*, CRC Press, Boca Raton, Florida, USA **2005**.
- [29] H. Günzler, H. Gremlich, *IR-Spektroskopie*, John Wiley & Sons, Ltd, Weinheim, Germany **2013**, p. 157.
- [30] J. Feltzin, M. K. Barsh, E. J. Peer, I. Petker, *J. Macromol. Sci.: Part A – Chem.* **1969**, *3*, 261.
- [31] M. K. Antoon, J. L. Koenig, *J. Polym. Sci., Polym. Chem. Ed.* **1981**, *19*, 549.
- [32] S. T. Cholake, M. R. Mada, R. K. S. Raman, Y. Bai, X. Zhao, S. Rizkalla, S. Bandyopadhyay, **2014**, *64*, 314–321.
- [33] L. Monney, R. Belali, J. Vebrel, C. Dubois, A. Chambaudet, *Polym. Degrad. Stab.* **1998**, *62*, 353.
- [34] B. Steinmann, *J. Appl. Polym. Sci.* **1989**, *37*, 1753.
- [35] F. N. Alhabill, R. Ayoob, T. Andritsch, A. S. Vaughan, *J. Mater. Sci.* **2018**, *53*, 4144.
- [36] V. T. Nguyen, A. S. Vaughan, P. L. Lewin, A. Krivda, *IEEE Trans. Dielectr. Electr. Insul.* **2015**, *22*, 895.
- [37] R. F. Fischer, *J. Polym. Sci.* **1960**, *44*, 155.
- [38] L. Matějka, J. Lövy, S. Pokorný, K. Bouchal, K. Dušek, *J. Polym. Sci., Polym. Chem. Ed.* **1983**, *21*, 2873.
- [39] J. Leukel, W. Burchard, R.-P. Krüger, H. Much, G. Schulz, *Macromol. Rapid Commun.* **1996**, *17*, 359.
- [40] A. I. Barabanova, B. V. Lokshin, E. P. Kharitonova, E. S. Afanasyev, A. A. Askadskii, O. E. Philippova, *Polymer* **2019**, *178*, 121590.
- [41] W. Fisch, W. Hofmann, J. Koskikallio, *J. Appl. Chem.* **1956**, *6*, 429.
- [42] G. C. Stevens, *J. Appl. Polym. Sci.* **1981**, *26*, 4279.
- [43] M. Jux, B. Finke, T. Mahrholz, M. Sinapius, A. Kwade, C. Schilde, *J. Nanopart. Res.* **2017**, *19*, 19.

SUPPORTING INFORMATION

Additional supporting information may be found online in the Supporting Information section at the end of this article.

How to cite this article: T. Waniek, U. Braun, D. Silbernagl, H. Sturm, *J Appl Polym Sci* **2021**, e51006. <https://doi.org/10.1002/app.51006>